Velocity Sensitivity of Reverse-time Migration

Guojian Shan, Lin Zhang, Yue Wang, Tamas Nemeth and Wei Liu, Chevron Energy Technology Company*

SUMMARY

We investigate the sensitivity of reverse-time migration (RTM) to migration velocity errors for prestack depth imaging. Based on the BP 2004 velocity benchmark, we add small errors to the velocity above top-of-salt and iterated on migration velocity analysis to compare the results from using several migration methods: conventional downward extrapolation, tilted plane-wave migration, and RTM. Our results show that RTM can be more sensitive to velocity errors than does one-way imaging when spurious reflections in RTM are misinterpreted to update in model building. In this experiment with imperfect velocities, we also observe that RTM and tilted plane-wave migration have less degradation in defining some subsalt structures compared to conventional downward continuation migration.

INTRODUCTION

Conventional downward continuation migration can not accurately image steeply dipping reflectors because of its dip limitation in handling waves that either propagate nearly horizontally or overturn in laterally varying media. Plane-wave migration in tilted coordinates (Shan and Biondi, 2004), although also based on the one-way wave equation, is capable of imaging steeply dipping reflectors by making the extrapolation direction close to the propagation direction. Reverse-time migration (Whitmore, 1983; Baysal et al., 1983; McMechan, 1983) based on the two-way wave equation has no dip limitation, but in general it is computationally more expensive than one-way imaging methods. In recent years, RTM draws increasing attention (Jones et al., 2007; Liu et al., 2007; Zhang et al., 2007), due to rapid advance in high performance computing capabilities.

Model driven imaging is an iterative process between migration and velocity estimation (Biondi, 2006). An important question is whether reverse-time migration is more sensitive to velocity errors compared to migration methods based on the one-way wave equation (Karazincir and Gerrard, 2007). In this study, we compare the velocity sensitivity of three migration methods: conventional downward continuation, plane-wave migration in tilted coordinates, and reverse-time migration. The comparisons are based on synthetic tests using the BP 2004 velocity benchmark (Billette and Brandsberg-Dahl, 2005).

MIGRATION METHODS

In conventional downward continuation migration, the source wavefield $S(s,x,z,\omega)$ and receiver wavefield $R(s,x,z,\omega)$ are extrapolated to the subsurface using the one-way wave equations,

$$\frac{\partial S}{\partial z} = +i\sqrt{\frac{\omega^2}{v^2}+\frac{\partial^2}{\partial x^2}}S \quad (1)$$

$$\frac{\partial R}{\partial z} = -i\sqrt{\frac{\omega^2}{v^2}+\frac{\partial^2}{\partial x^2}}R \quad (2)$$

where s is the source location, x is the horizontal location, z is the vertical location, and ω is circular frequency. The image for the shot at s, $I(s,x,z)$ is generated by cross-correlating the source and receiver wavefields as follows:

$$I(s,x,z) = S^*(s,x,z,\omega)R(s,x,z,\omega), \quad (3)$$

where S^* is the complex conjugate of S. The one-way wavefield extrapolation operator cannot accurately propagate waves in a direction far from the extrapolation direction, such as nearly horizontal directions in downward continuation. In addition, the one-way extrapolator is not designed to handle overturned waves and prismatic waves. The dip limitation can be remedied by using plane-wave migration in tilted coordinates, which makes extrapolation direction close to the propagation direction.

In reverse-time migration, source and receiver wavefields can be extrapolated along the time axis by solving the two-way wave equation:

$$\frac{1}{v^2}\frac{\partial^2 P}{\partial t^2} = \frac{\partial^2 P}{\partial x^2}+\frac{\partial^2 P}{\partial z^2} \quad (4)$$

where P can be either source wavefield $S(s,x,z,t)$ or receiver wavefield $R(s,x,z,t)$. The image of the shot at s, $I(s,x,z)$ is generated by cross-correlating the source and receiver wavefields as follows:

$$I(s,x,z) = \sum_t S(s,x,z,t)R(s,x,z,t). \quad (5)$$

Unlike one-way imaging, the two-way wave extrapolator can handle waves propagating in any direction, including overturning waves, prismatic waves, and multiples. The more complete set of events that can be handled by RTM may not be well imaged if velocity and imaging condition are not properly tuned to focus these events.

A SINGLE HORIZONTAL REFLECTOR MODEL

The first synthetic model consists of two homogeneous layers (Figure 1): a slow sedimentary layer (P-wave velocity 2 km/s) overlying on a fast salt layer (4.5 km/s). Velocity contrast between the two layers is located at depth 2 km.

Figure 2 shows images obtained by migrating a single shot-gather using the correct velocity. Panels (a) and (b) are obtained by downward continuation migration and RTM, respectively. The reflectors in the two images are comparable, except

Downloaded 11 Jun 2011 to 128.12.131.6. Redistribution subject to SEG license or copyright; see Terms of Use at http://segdl.org/

that RTM generates smooth back-scattering noise in panel (b), which can be eliminated largely by a low-cut filter or more completely by using a directivity-based imaging condition. Figure 3 shows the images using an incorrect velocity model where the top salt is located at 1.95 km instead of 2 km. This change makes the average velocity faster for migrating the reflection. As a result, the reflection event gets overmigrated and moves below 2 km. In Figure 3(b), in addition to the overmigrated event, there is another mirror event above 2 km as a result of spurious reflections from the mispositioned velocity contrast at 1.95 km. The spurious reflections can occur in both source and receiver wavefields at the contrast and are cross-correlated into the mirror image.

It is noticeable that velocity errors complicate the back-scattering noise even in this simple test. The high-frequency components in the back-scattering noise cannot be removed effectively by a low-cut filter. A directivity-based imaging condition is more suited for removing the noise.

These comparisons indicate that with imperfect velocity models, the transmission components of both migration methods behave similarly, yet RTM can be more sensitive to the positioning accuracy of strong impedance contrasts. Spurious reflections in RTM due to interface positioning errors may lead to misinterpretation if they are not properly identified and addressed in imaging.

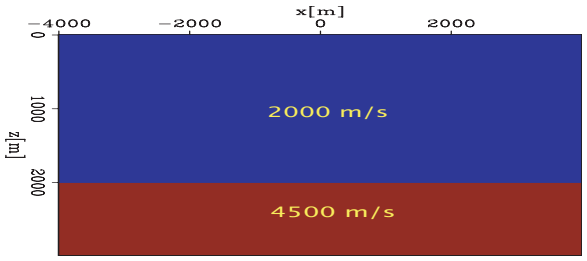

Figure 1: The velocity model of the two-layer media.

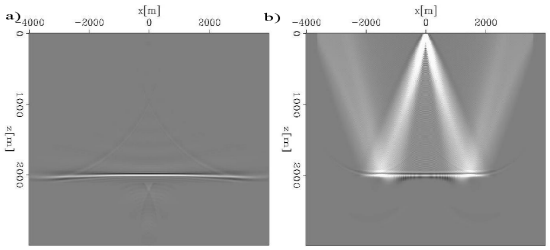

Figure 2: Migration with the correct velocity: (a) downward continuation migration; (b) reverse-time migration.

THE BP 2004 VELOCITY BENCHMARK

The BP 2004 velocity model (Figure 4) was designed to benchmark velocity estimation accuracy (Billette and Brandsberg-Dahl, 2005). It is a composed section representing challenging

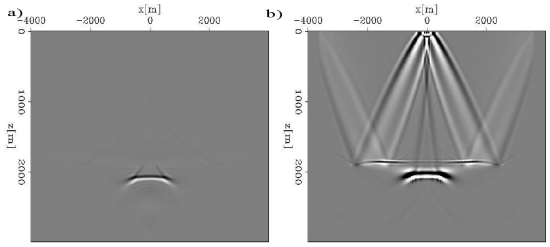

Figure 3: Migration with mispositioned top-of-salt: (a) downward continuation migration; (b) reverse-time migration.

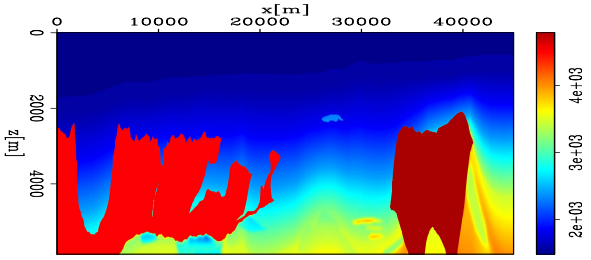

Figure 4: The correct velocity model.

deepwater structures from different parts of the world. Imaging the steeply dipping salt flanks in this section is a significant challenge for conventional downward continuation migration. However, these salt flanks can be well imaged by RTM and plane-wave migration in tilted coordinates (Shan and Biondi, 2006).

Figure 5 shows images obtained by migrating the dataset using the correct velocity. Panels (a), (b) and (c) correspond to results from downward continuation migration, plane-wave migration in tilted coordinates and RTM, respectively. Steeply dipping salt flanks and rugose salt top are either not imaged or incorrectly positioned in panel (a); whereas they are well imaged in panels (b) and (c). It is also noticeable that low-cut filtering eliminates largely the back-scattering noise in panel (c). The noise elimination can be further improved by using a directivity-based imaging condition.

To simulate migration velocity analysis (MVA) in which the starting model is often imperfect, we introduced velocity errors that is less than 4% to the sediments above top-of-salt. Figure 6 shows the error percentage in the velocity model. We first ran a sediment velocity flooding, and picked top-of-salt following an prestack depth migration. With top-of-salt fixed, we ran a salt flooding, and picked base-of-salt following a second migration. We did several iterations of sediment and salt flooding to finalize on the salt geometry in the multi-value areas. Finally we inserted the true sub-salt velocity back into our migration model and use it for the final run of migration.

Figure 7 shows images based on the final velocity out of the above model building procedure. Similar to Figure 5, steeply dipping salt flanks are not well imaged by conventional downward continuation in panel (a), but they are well focused by tilted plane-wave migration in panel (b) and RTM in panel (c).

Downloaded 11 Jun 2011 to 128.12.131.6. Redistribution subject to SEG license or copyright; see Terms of Use at http://segdl.org/

The back-scattering noise in Figure 7(c) appears to be more complex than that in Figure 5(c). Such back-scattering noise is not effectively eliminated by low-cut filtering. A directivity based imaging condition may be more effective. At location "A" near a large salt canyon (Figure 7(c)), it is visible that top-of-salt splits into two horizons, similar to the dual top-of-salt images in Figure 3(b). At location "B", the thick bottom of the salt canyon experiences wavelet overlapping from the dual top-of-salt events. The distance between the overmigrated top-of-salt and its mirror image can be diagnostic of the error in top-of-salt positioning. In this case, the local thickening top-of-salt indicates close proximity of dual events and small velocity errors.

We further look into the consequence of picking spurious horizons in iterative model building. In Figure 8, we can also observe the characteristic top-of-salt splitting at locations "A" and "B". The ghosting top-of-salt (the top one) is generated from the reflections of source and receiver wavefields at the salt boundary. This mirror image has stronger focusing than the overmigrated one below, therefore appears to be the "true" salt boundary. But if the ghosting horizon is mistakenly picked as top-of-salt to update, the interpreted top-of-salt would be biased away from the actual location throughout iterations. Therefore, picking the ghosting top-of-salt in velocity update could lead to divergence in salt geometry delineation.

Figure 9 shows sub-salt images using an incorrect velocity model with errors in both sediments and salt bodies. The salt geometry in the model is picked based on the output from plane-wave migration in tilted coordinates. Most subsalt structural images are comparable in three panels, but in some areas (highlighted in rectangles), certain reflectors suffer less degradation in panels (b) and (c) than do those in panel (a).

CONCLUSION

Both reverse-time migration and one-way migration methods have similar sensitivity to velocity errors in handling one-way propagation. However, if major impedance contrasts are misspecified in migration models, reverse-time migration can generate spurious reflections and mirror images with apparently strong focusing. These spurious mirror images, if misinterpreted as horizons to update, could lead to divergence in model building. In this sense, reverse-time migration can be more sensitive to the positioning accuracy of strong impedance contrasts when compared with one-way migration methods. In this specific synthetic experiment with imperfect velocities, we also observe that reverse-time migration and plane-wave migration have less degradation in imaging some parts of subsalt structures than does conventional downward continuation migration.

ACKNOWLEDGMENTS

We thank Chevron Energy Technology Company for permission to publish this paper. We also thank BP for making the synthetic dataset available.

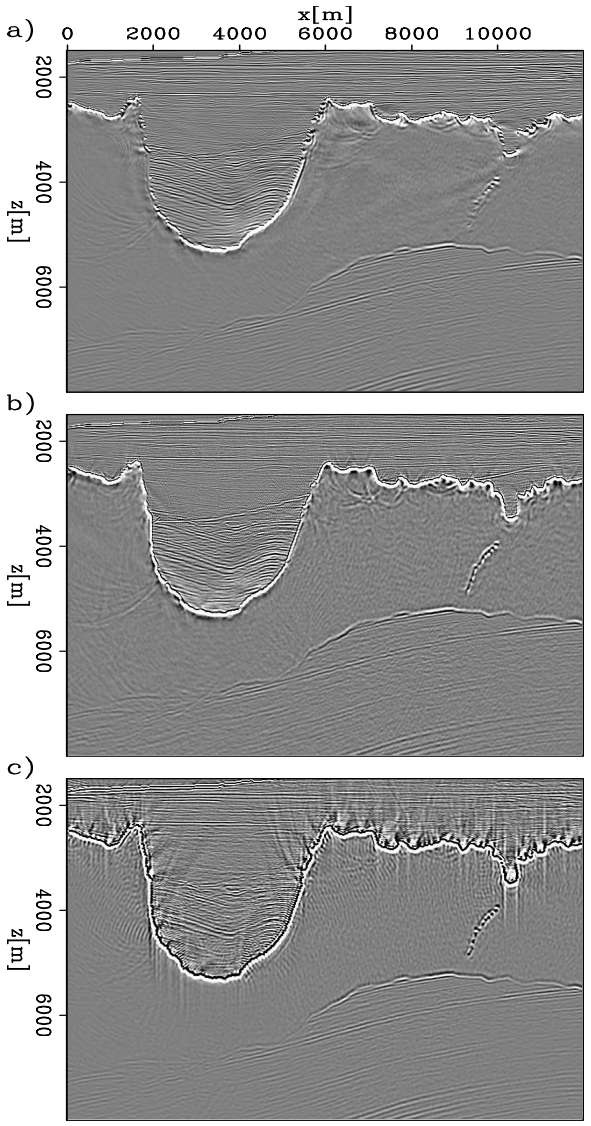

Figure 5: PSDM based on the correct velocity model: (a) downward continuation; (b) plane-wave migration in tilted coordinates; (c) reverse-time migration (the back-scattering noise elimination can be further improved by using a directivity-based imaging condition).

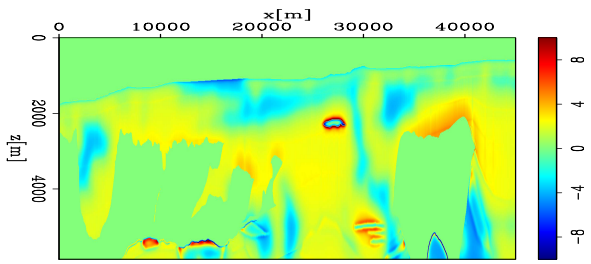

Figure 6: Velocity error percentages in sediments.

Downloaded 11 Jun 2011 to 128.12.131.6. Redistribution subject to SEG license or copyright; see Terms of Use at http://segdl.org/

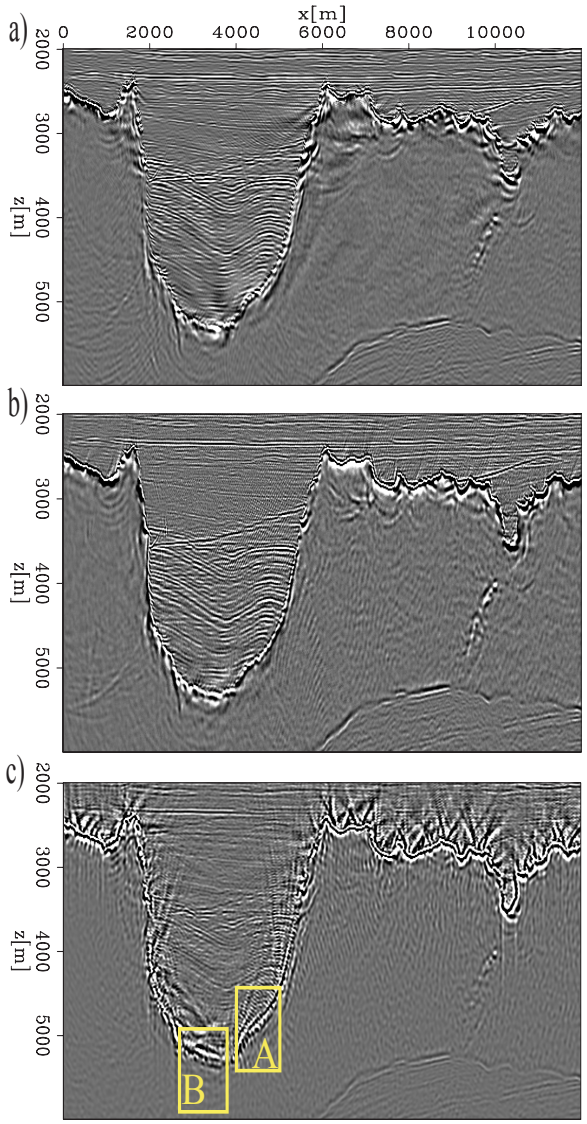

Figure 7: PSDM based on an iterated velocity model with errors: (a) downward continuation; (b) plane-wave migration in tilted coordinates; (c) reverse-time migration.

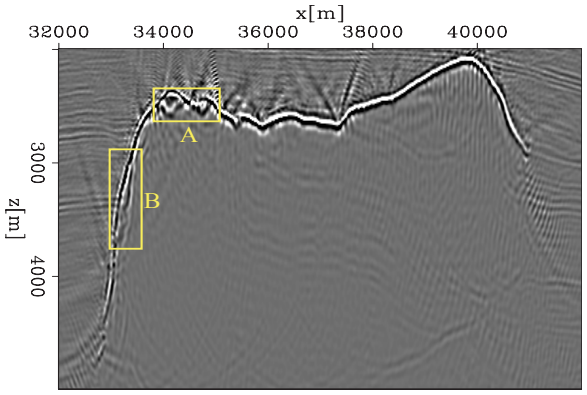

Figure 8: If salt geometry is not well picked, reverse-time migration generates dual salt boundaries.

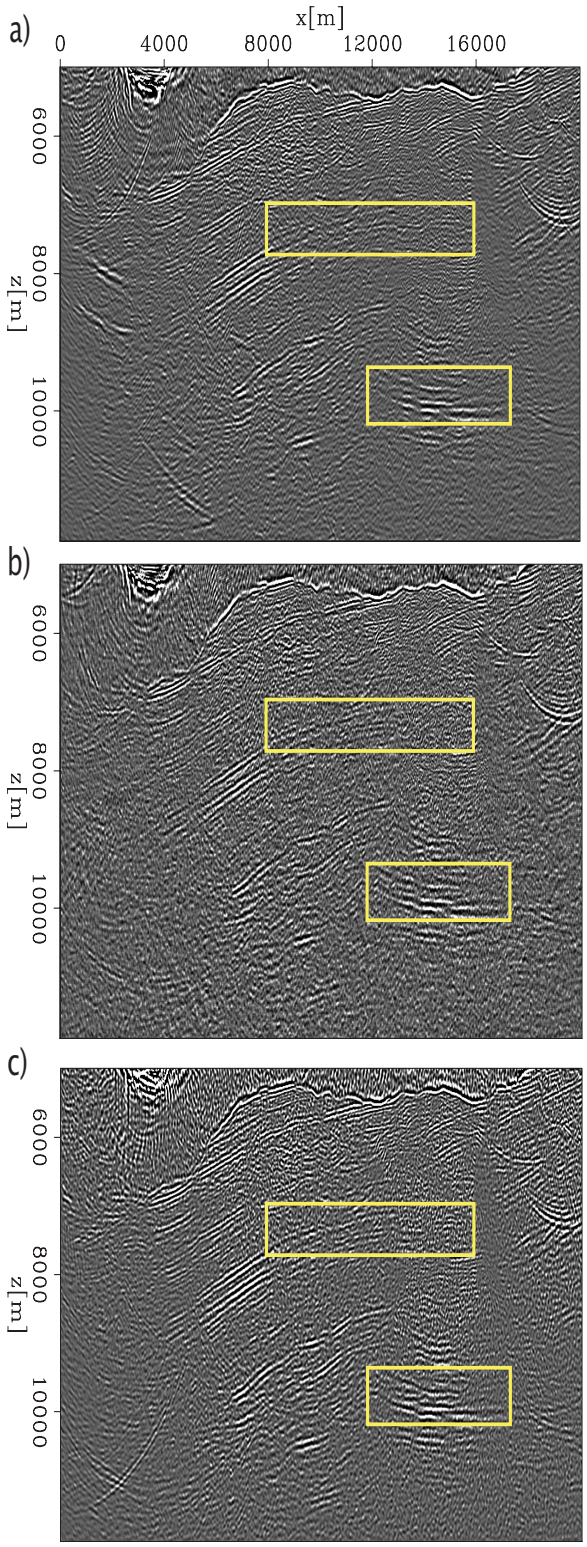

Figure 9: Comparison of sub-salt images based on an MVA-derived velocity model with errors: (a) downward continuation; (b) plane-wave migration in tilted coordinates; (c) reverse-time migration.

Downloaded 11 Jun 2011 to 128.12.131.6. Redistribution subject to SEG license or copyright; see Terms of Use at http://segdl.org/

EDITED REFERENCES

Note: This reference list is a copy-edited version of the reference list submitted by the author. Reference lists for the 2008 SEG Technical Program Expanded Abstracts have been copy edited so that references provided with the online metadata for each paper will achieve a high degree of linking to cited sources that appear on the Web.

REFERENCES

Baysal, E., D. D. Kosloff, and J. W. C. Sherwood, 1983, Reverse time migration: Geophysics, **48**, 1514–1524.

Billette, F., and S. Brandsberg-Dahl, 2005, The 2004 BP velocity benchmark: 67th Annaul International Conference and Exhibition, EAGE, Extended Abstracts, B035.

Biondi, B., 2006, Three dimensional seismic imaging: SEG.

Jones, I. F., M. C. Goodwin, I. D. Berranger, H. Zhou, and P. A. Farmer, 2007, Application of anisotropic 3D reverse time migration to complex north sea imaging: 77th Annual International Meeting, SEG, Expanded Abstracts, 2140–2144.

Karazincir, M. H., and C. M. Gerrard, 2007, Two-way versus one-way wave-equation PSDM velocity sensitivity: 77th Annual International Meeting, SEG, Expanded Abstracts, 2305–2309.

Liu, F., G. Zhang, S. A. Morton, and J. P. Leveille, 2007, Reverse-time migration using one-way wavefield imaging condition: 77th Annual International Meeting, SEG, Expanded Abstracts, 2140–2144.

McMechan, G. A., 1983, Migration by extrapolation of time-dependent boundary values: Geophysical Prospecting, **31**, 413–420.

Shan, G., and B. Biondi, 2004, Imaging overturned waves by plane-wave migration in tilted coordinates: 74th Annual International Meeting, SEG, Expanded Abstracts, 969–972.

———2006, Imaging steep salt flank with plane-wave migration in tilted coordinates: 76th Annual International Meeting, SEG, Expanded Abstracts, 2372–2376.

Whitmore, N. D., 1983, Iterative depth migration by backward time propagation: Presented at the 53rd Annual International Meeting, SEG.

Zhang, Y., G. Zhang, D. Yingst, and J. Sun, 2007, Explicit marching method for reverse-time migration: 77th Annual International Meeting, SEG, Expanded Abstracts, 2300–2304.

Downloaded 11 Jun 2011 to 128.12.131.6. Redistribution subject to SEG license or copyright; see Terms of Use at http://segdl.org/